IIETA International Information and Engineering Technology Association
Advancing the World of Information and Engineering

Traitement du Signal
Vol. 40, No. 2, April, 2023, pp. 479-490
Journal homepage: http://iieta.org/journals/ts

4^{th} Order Shannon Energy Envelope Approach for Localization of S_1 and S_2 for Early-Stage Detection of Heart Valve Dysfunction

Madhwendra Nath*, Subodh Srivastava

Department of Electronics and Communication Engineering, National Institute of Technology Patna, Patna 800005, India

Corresponding Author Email: madhwendran.phd19.ec@nitp.ac.in

https://doi.org/10.18280/ts.400207

Received: 10 November 2022
Accepted: 17 March 2023

Keywords:
empirical mode decomposition (EMD), modified Shannon energy envelope (MSEE), combined component signal, PCG, ECG, cardio vascular diseases (CVD)

ABSTRACT

The recent reports of the World Health Organization showed that a huge extent of the population below 55 years has become much prone to cardiac disease, and the death percentage has increased caused by various cardio vascular diseases (CVD). Moreover, in the Covid-19 pandemic situation, the people suffering from heart disease were found severely vulnerable to viral infections, which proved to be a major cause of increased death percentage. The CVD could be caused by dysfunction of heart valves which could end up with cardiac arrest. The prime method for early-stage detection of the heart valve dysfunction is analysis of major heart sounds occurring in a cardiac cycle. The proposed work dealt with exploration of S_1 and S_2, which are supposed to be prime sounds of Phonocardiogram (PCG) signal. Here, the proposed analysis has six steps. First, signal-acquisition set-up which was assembled for acquiring PCG and ECG signals from the people having age between 15 to 40 years. Second step, pre-processing: in which the samples of PCG and ECG signals were prepared and the signal was denoised using modified Butterworth worth filter. The third step was the incorporation of Empirical Mode Decomposition to get Intrinsic Mode Functions i.e., frequency components of the PCG. Further, only two appropriate IMFs were selected and recombined to generate a combined component signal (CC_{hs}). In the fourth step; a Modified Shannon Energy Envelope algorithm (MSEE) i.e., 4th order Shannon energy Envelope was implemented to frame energy envelopes. In the fifth step; an adaptive-thresholding was used for the time-lobes formation followed by peak correction algorithm i.e., correction of time-lobe peaks. In the sixth and final step; time-lobes of the PCG signal were computed and were correlated with R-peaks of ECG signal, through which localization of S_1 and S_2 was done. A total of 40 samples of the PCG signal consisting of 195 cardiac cycles were taken for the analysis. It came out from the analysis of the self-acquired PCG signal that the best result of localization of S_1 and S_2 is obtained for the PCG signal acquired from the Pulmonic position. After analyzing the confusion matrix for the findings of the proposed method; accuracy & precision were 90.20%, sensitivity 100%, and an error rate of 9.8% was obtained. The accuracy of the method was found lesser if the PCG was acquired from the remaining three auscultation areas of the human chest. The proposed method was compared with three other earlier algorithms, out of which the proposed method showed a greater improvement. Moreover, the implementation of EMD followed by choosing a few specific IMFs for the formation energy envelope reduced the computation cost and enhanced the accuracy of the method, too.

1. INTRODUCTION

The latest WHO reports revealed that in 2019 heart disease caused deaths of more than 17 million population of the world which accounts for 32% of all global deaths in the year [1]. In 2016 in India, 27% of reported deaths were caused by cardiovascular disease (CVD) out of which 45% of people who lost their lives were of age group 40-69 years [2]. In the last few years, one-fifth of the total deaths in India were deaths caused by heart disease. And this happened especially in the working-age population below the age of 55 years (Report: The Indian Express, 29th Sept 2021). Moreover, in the COVID-19 pandemic situation, a few studies showed that the mortality rate of CVD patients due to covid-19 was 14% higher and could be up to 87%. Therefore, time demands to focus more on the detection of early-stage symptoms of heart disease to curb the mortality rate. Sometimes, a few heart diseases are caused by dysfunction of the heart valve which could result into some issues inside the heart like back-flow of blood across the heart chambers, leaking of blood through narrow openings. These issues could lead to a sudden cardiac arrest. The early-stage detection and diagnosis of such cardiac problems is possible by analysis of the PCG signal. Such analysis identifies the heart-valve-dysfunction at early-stage and can reduce the risk of cardiac arrest. It is an interesting fact that the first heart sound S_1 and the second heart sound S_2 have larger amplitude-variation, so the level of information would be greater in these two sounds, obviously. On the other hand, the S_3 and S_4 have lesser amplitude-variation and most of the times they get merged with the noises and the heart murmurs. Therefore, the analysis of S_1 and S_2 gives much satisfactory results of diagnosis.

For identification of S_1 and S_2; Liang et al., presented a method based on heart sound envelogram. Although this algorithm detected the S_1-S_2 with 93% accuracy, the algorithm was found noise-sensitive [3]. An adaptive-thresholding based approach for localization of S_1 and S_2 was proposed by Belmecheri et al., but a loss of information was found due to the computational complexity of the method [4]. Bajelani et al. made an effort to detect S_1 and S_2 based on empirical mode decomposition in which the accuracy of detection of S_1-S_2 was shown 88.3%, but the method was too noise-prone [5]. In another approach; effort was made for identification of S_1 and S_2 by Nath et al. where PCG consist of 2520 cardiac cycles were taken but added extra noise was observed at the pre-processing stage of the method [6]. Narváez et al. adopted an approach for segmentation of heart sound based on modified empirical wavelet transform which showed an accuracy of 99.26%, but the method reflected several differences from manually segmented findings [7]. Again, Nath et al. made an effort for detection of S_1-S_2, but noise-sensitivity of the method revealed accuracy up to 74%, only [8]. Liu et al. proposed an approach for an automatic segmentation of S_1, S_2, S_3, and S_4 in which an Automatic low pass filter (ALPF) was used to separate murmurs. Here, an accuracy of detection was found 98.49%, but the method was found inappropriate for the heart signal with severe arrhythmia [9]. Akram et al. made an effort for localization of S_1 and S_2 using homomorphic filtering for which they achieved an accuracy of localization upto 97%, but it failed in accurate localization for corrupted heart sound signal [10].

Generally, the popular methods for monitoring of human heart are Electrocardiogram and blood test. But, for the valvular-heart-disease; non-invasive acoustic sensors are used to record Phonocardiogram (PCG). The PCG is recorded by placing an acoustic sensor or electronic stethoscope on any of the four auscultation points of the human chest i.e., Pulmonic, Aortic, Mitral, and Tricuspid positions. Appropriate placement of heart sound sensor on specified auscultation area of the human chest gives-out more accurate PCG signal [11-15].

The proposed analysis has six steps: very first, the Phonocardiogram and the Electrocardiogram signal were acquired. The Phonocardiogram was acquired using an electronic stethoscope by placing it on every location of bare human-chest i.e., Pulmonic, Aortic, Mitral, and Tricuspid. The Second step was pre-processing; in which samples of PCG and ECG signals were prepared of time length 5-8 seconds consisting of 6-10 cardiac cycles. Then, the signal was de-noised using Modified Butterworth filter. Third, a decomposition of PCG signal was done by incorporation of Empirical Mode Decomposition which came out with 8-12 frequency constituents the PCG signal. Each frequency constituent is called as Intrinsic Mode Function (IMF). Further, out of 8-12 IMFs only first two IMFs i.e., first two frequency constituents were taken and recombined to create combined component signal (CC_{hs}). Fourth; a Modified Shannon Energy Envelope algorithm (MSEE) i.e., a 4^{th} order Shannon energy envelope method was implemented on the combined component signal (CC_{hs}) for creation of energy envelope. Fifth; an adaptive-thresholding was used for time-lobe formation followed by peak-correction algorithm i.e., correction of time-lobe-peaks. Sixth; the time-lobes obtained from PCG signal and R-peaks obtained of ECG signal was computed and a correlation was established to localize the S_1 and S_2. The proposed work was compared with three other pre-existing methods.

2. METHODS AND MODELS

The proposed work explores an algorithm based on Empirical Mode Decomposition (EMD) and Modified Shannon Energy Envelope method i.e., 4^{th} order Shannon energy for localization of S_1-S_2. The PCG signal was acquired from persons of age group 15-40 years. It was a self-acquired signal; each signal recording was of length 2-3 minutes. From every subject, the PCG signal was acquired by placing the electronic stethoscope on Tricuspid, Aortic, Mitral, and Pulmonic positions of the bare chest of a person. Particularly, for the proposed analysis; 10 samples (each of time length 5-10 seconds) from each auscultations area were taken i.e., total 40 samples were taken. It was consisting of total 195 cardiac cycles. The proposed algorithm was implemented as per following flow chart in Figure 1.

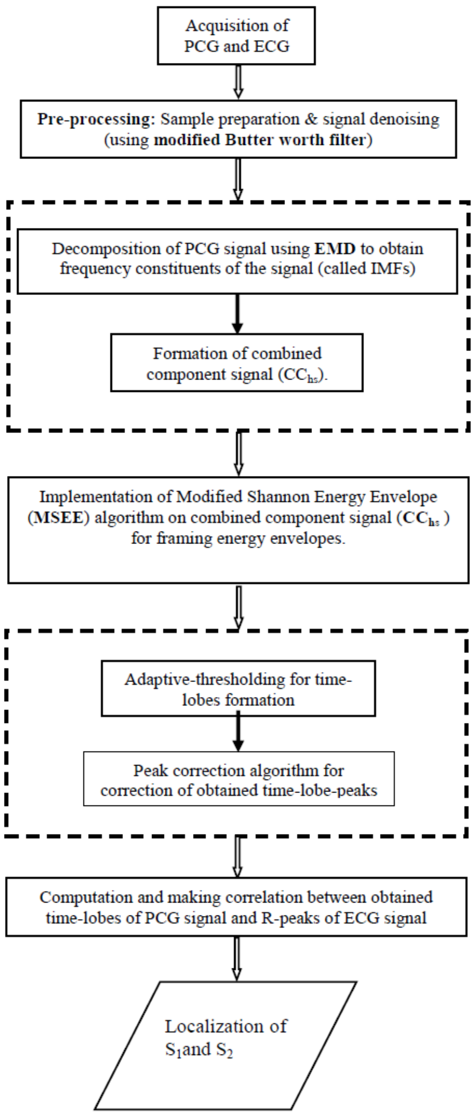

Figure 1. Steps of the proposed methodology (i.e., from acquisition of the signal to localization of S_1-S_2)

2.1 System set-up and signal acquisition

The very first part was the acquisition of the PCG i.e., Heart Sound signal. It was much crucial part. The subject was made relaxed for minimum 10 minutes before the signal acquisition. Thereafter, the electronic stethoscope SS30L was placed in an appropriate position on the chest of the subject. ECG signal was also recorded in parallel by using 3-limb electrodes.

An MP36 system set-up (of BIOPAC System Inc.) was used for the acquisition of Phonocardiogram and Electrocardiogram signals. For the PCG, an electronic stethoscope (SS30L) was used whereas for the acquisition of the ECG a lead set (SS2LA/L) was used along with EL503. Both the signals were recorded at a sampling frequency of 5000 samples/second [16].

The PCG and the ECG signals of 40 persons were acquired as per the experimental setup shown in Figure 2. Moreover, as per the declaration of Helsinki, written consent was taken from every volunteer to take their biological data and use it for research and analysis purposes. The computer system was consisting of BIOPAC BSL PRO software through which the acquired signal was saved into excel and .txt format for further analysis in MATLAB.

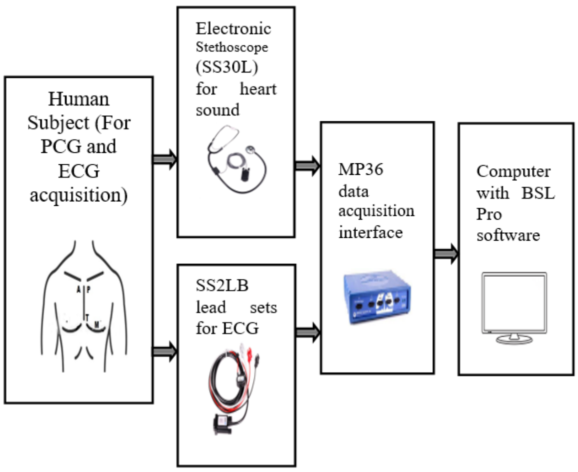

Figure 2. Experimental set-up for recording of the signal (Images courtesy: biopac.com [16]). To record the heart sound, the electronic stethoscope (SS30L) was placed at P, A, M, T positions of human chest. For ECG recording SS2LB lead set was used. Both the data were taken into a computer using the MP36 interface

2.2 Sample preparation and pre-processing

Each signal sample that was cropped from the acquired data was of length 4-10 seconds and was consisting of 4-8 cardiac cycles. Further, the signal was re-sampled to a sampling frequency 1000Hz, as it made the signal better-ready for the proposed analysis method. Afterward, the signal was normalized then signal cleaning was done by applying a modified Butterworth filter i.e., signal was passed through low-pass-Butterworth-filter (F_c=200 Hz, Orde=8) and high-pass-Butterworth-filter (F_c=20 Hz, Orde=5), back to back. This filtering action removed the low-frequency artefacts and high-frequency noises at an adequate amount.

2.3 Empirical mode decomposition (EMD) of PCG signal and creation of CC_{hs}

The generation PCG signal involves very complex mechanism and is non-stationary signal. Therefore, it could be supposed as a multi-component signal. So, the Empirical mode decomposition (EMD) could decompose it into its frequency constituents, called Intrinsic Mode Functions (IMFs) [6, 17].

Now, the EMD was implemented on the PCG signal to decompose it into its frequency components called, Intrinsic-mode-function i.e., IMF-1, IMF-2, IMF-3, IMF-4, etc. Then, the frequency spectrum of each IMF was drawn and compared. After recombining the first two frequency components (i.e. IMF-1 and IMF-2, respectively) and regenerating a combined component signal (CC_{hs}) i.e. CC_{hs}=(IMF-1)+(IMF-2), It was found that the frequency spectrum of CC_{hs} was much resembling that of S_1-S_2 i.e. 20-200 Hz [7, 18]. As the proposed analysis was confined to the analysis of S_1-S_2, therefore the combined component signal (CC_{hs}) was generated from each sample of PCG signal and was used for further steps of the proposed analysis. It reduced the computational cost as well as rescued from high-frequency noise and low-frequency artefacts.

2.4 Implementation of 4th order Shannon energy envelope approach on combined component signal (CC_{hs})

The earlier literature showed that if the Shannon Energy envelope method is used directly for the heart sound analysis, it could lead to false segmentation; as it is sensitive to the heart murmurs [8]. Now, a modified Shannon Energy Envelope algorithm (MSEE) i.e., 4th order Shannon Energy Envelope approach was implemented on combined component signal (CC_{hs}). The standard formula for Shannon energy is as following [3]:

$$E_S = -\frac{1}{N}\sum_{i=1}^{N} x^2(i) * \log x^2(i) \qquad (1)$$

where, $x\ (i)$=Normalized Original Signal, E_s =Normalized average Shannon Energy.

But the 4th order modified Shannon energy formula is as following:

$$\boldsymbol{E_{MS} = -\frac{1}{N}\sum_{i=1}^{N} x^4(i) * \log x^4(i)} \qquad (2)$$

In this work, the Modified Shannon Energy Envelope formula (MSEE) i.e., 4th order Shannon Energy formula was used for the formation of smoother energy envelopes.

2.5 Time-lobe formation through adaptive-thresholding and correction of time-lobe-peaks

The framed energy envelops were consisting of various peaks. Generally, two higher peaks per cardiac cycle were observed in the obtained energy envelope. It had a higher possibility that these two higher peaks per cardiac cycle could be indicating the time-lobe position of S_1 and S_2 i.e., most expected positions of finding of S_1 and S_2. Therefore, an automatic-thresholding algorithm was implemented to get the Time-lobes (i.e., time-segments) for localization of S_1 and S_2. The thresholding algorithm which was based on the Cubic-spline concept, computed a “unique threshold point” for each inserted signal [8]. Finally, the Time-lobes were created from the energy envelope.

Correction of time-lobe-peaks

In certain signals, a few undesired time-lobes were get appeared or some desired time-lobes were get suppressed, leading to false detection. To endure this situation, a peak correction algorithm, based on modified median filtering was incorporated [19].

2.6 Correlating the time-lobes of PCG signal with R-peaks of ECG signal and localization of S_1 and S_2

Since the ECG signal was simultaneously acquired just to infer the number of cardiac cycles taken in the sample. During one cardiac cycle of ECG signal only one R-peak. Therefore, the computation of R-peaks in the given ECG sample could come up with the number of cardiac cycles taken in the sample. This calculation could be helpful in the localization of S_1 and S_2 in the final step.

For the detection and computation of R-peaks in the simultaneously acquired ECG signal following process was implemented:

a) ECG signal cleaning using the same Modified Butterworth filter.

b) Implementation of Modified Shannon Energy Envelope algorithm (MSEE) on the ECG signal for the creation of an energy envelope.

c) Further, the same adaptive-thresholding method was incorporated into energy envelopes of ECG for time-lobes formation. These time-lobes infer the time-stamps of R-peaks in the Electrocardiogram.

As the R-peak of the ECG signal has adequate high amplitude, the R-peaks of the Electrocardiogram signal is detected easily with the said method. And, one time-lobe-peak per cardiac cycle is obtained from the ECG signal.

In an ideal situation, after incorporating the proposed method; a single time-lobe-peak per cardiac cycle should come out from the ECG signal inferring the location of the R-peak and two time-lobe-peaks per cardiac cycle would be obtained from the PCG signal indicating the location of S_1 and S_2 for a given sample. But during practical analysis, it did not happen frequently with the PCG signal, as there could be time-lobe-peak suppression or false detection of extra peaks. Because, the PCG signal, which was primarily acquired as an acoustic signal is a non-stationary and noise-prone signal, too. On the other hand, the ECG signal, which was acquired primarily as an electrical signal, was least vulnerable to noise and most of the time came up with a single time-lobe per cardiac cycle concerned to the R-peak. This was the main reason for taking the ECG as a reference signal for the proposed algorithm [8]. In further steps of the processing, this concept was used to correlate and to localize the S_1 - S_2. For example, the number of time-lobe peaks that came out from the CC_{hs} signal could be two-timed the number of time-lobe peaks detected from the ECG signal. Moreover, the position S_1-time-lobe-peak should be aligned with the position of time-lobe-peak concerned to R-peak. This phenomenon was exploited for the decision algorithm of successful localization of S_1 and S_2.

3. RESULTS AND DISCUSSION

3.1 Implementation and analysis

3.1.1 Sample preparation and pre-processing

In the proposed work, the signals were acquired at a sampling frequency of 5000 samples/second. As the maximum frequency range of desired heart sounds never exceed 500 Hz. Therefore, by the consideration of the Nyquist-theorem the signal was down-sampled i.e., re-sampled to 1000 samples/second. This down-sampling helped to reduce the processing time of the proposed method, too [5, 9]. Then, signal cleaning and denoising were done by using the Modified Butterworth filter. This means, first the signal was passed through the low-pass-Butterworth-filter (Fc=200Hz, Order=8) then it was passed through high-pass-Butterworth-filter (Fc=20 Hz, Order=5). The acquired ECG and PCG signals are displayed in Figure 3. Generally, the heart's sound is listened by medical practitioners using simple stethoscope. But if the heart sound signal which is recorded or acquired using electronic stethoscope and is taken into a computer system; is called as Phonocardiogram (PCG). Further, to normalize the signal, it was divided by its absolute value of maximum.

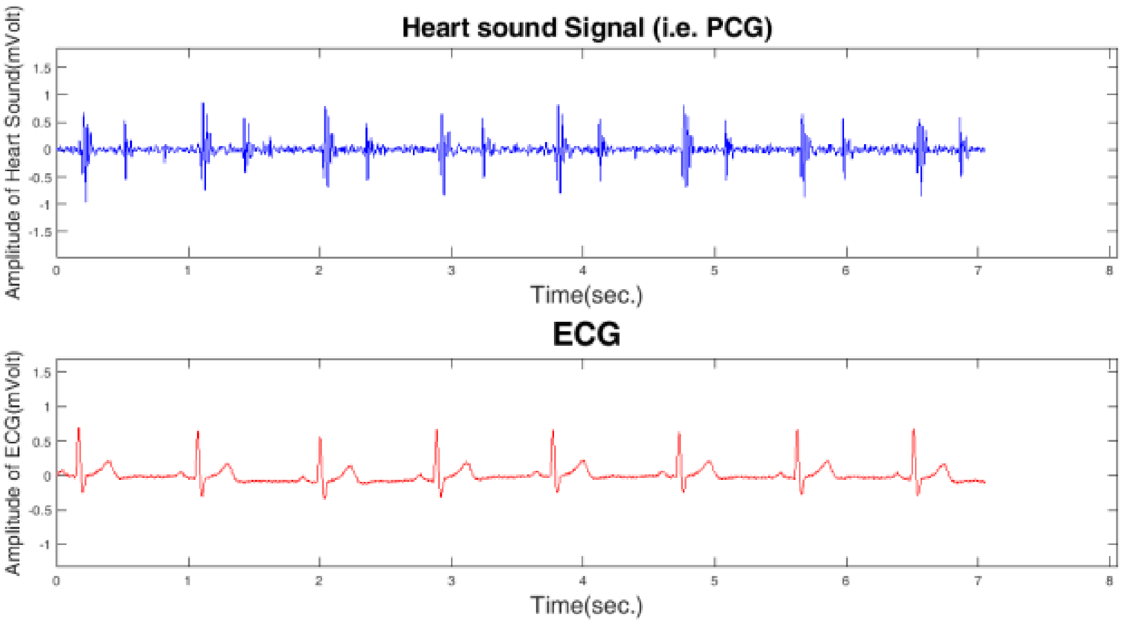

Figure 3. Acquired heart sound signal (i.e., PCG signal) and Electrocardiogram (ECG) signals i.e., first image (upper one) is of PCG signal and Second image (lower one) is simultaneously recorded ECG signal

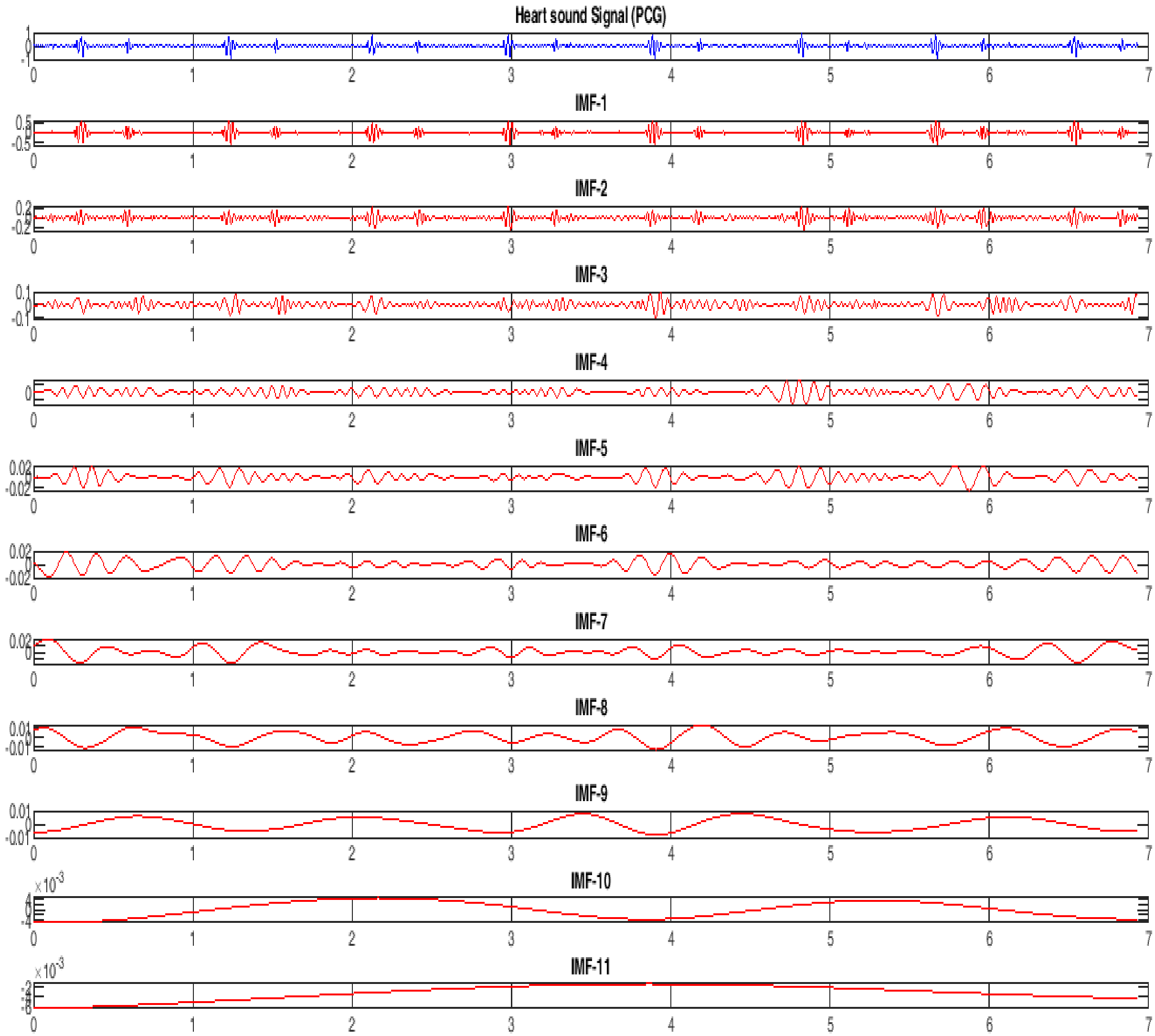

Figure 4. PCG signal and its frequency constituents (i.e., IMFs). The original heart sound signal (PCG) is at the top. And, from IMF-1 to IMF-11 are Intrinsic Mode Functions i.e., frequency constituents of the heart sound signal

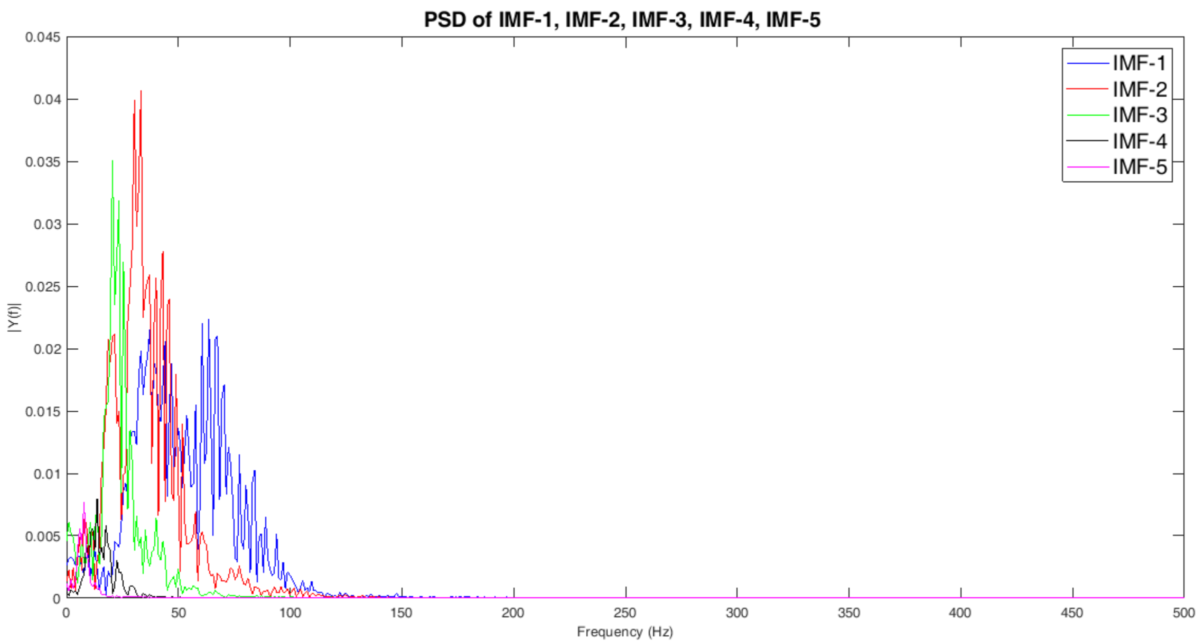

Figure 5. The frequency spectrum of IMF-1, IMF-2, IMF-3, IMF-4, and IMF-5

3.1.2 Empirical mode decomposition of PCG signal

Now, the Empirical mode decomposition algorithm was implemented on the PCG signal to decompose it into its frequency constituents. These frequency constituents are called, Intrinsic Mode Function (IMF). With the variation of frequency ranges of the obtained IMFs; these were named: IMF-1 (first frequency constituent), IMF-2 (second frequency constituent), IMF-3 (third frequency constituent), and IMF-4 (fourth frequency constituent), etc. Generally, 6-11 IMF i.e., frequency constituents were obtained after decomposition of every signal in the order of variation of higher frequency component to lower frequency component of the signal, from IMF-1 to IMF-11, respectively. The very last IMF was called a residue, as it contains very-low-frequency components. The PCG signal and its IMFs are displayed in Figure 4.

Further, the frequency spectrum of the PCG signal and its IMFs were obtained (as shown in Figure 5) and was analyzed. It was observed that if we take IMF-1 and IMF-2 and recombine it; then obtained combined component signal (CC_{hs}) had much resemblance of frequency range with that of S_1 and S_2. It can be more clearly observed from Figure 6 and Figure 7. Now, the combined component signal CC_{hs} was taken for the further steps of analysis as:

$$CC_{hs} = (IMF\text{-}1) + (IMF\text{-}2) \qquad (3)$$

3.1.3 Incorporation of the 4th order Shannon energy envelope method on CC_{hs}

Now, the 4th order Shannon Energy Envelope approach i.e., modified Shannon Energy Envelope method (MSEE) was incorporated to make energy envelope from the combined component signal (CC_{hs}). The energy envelope formed, is shown in Figure 8.

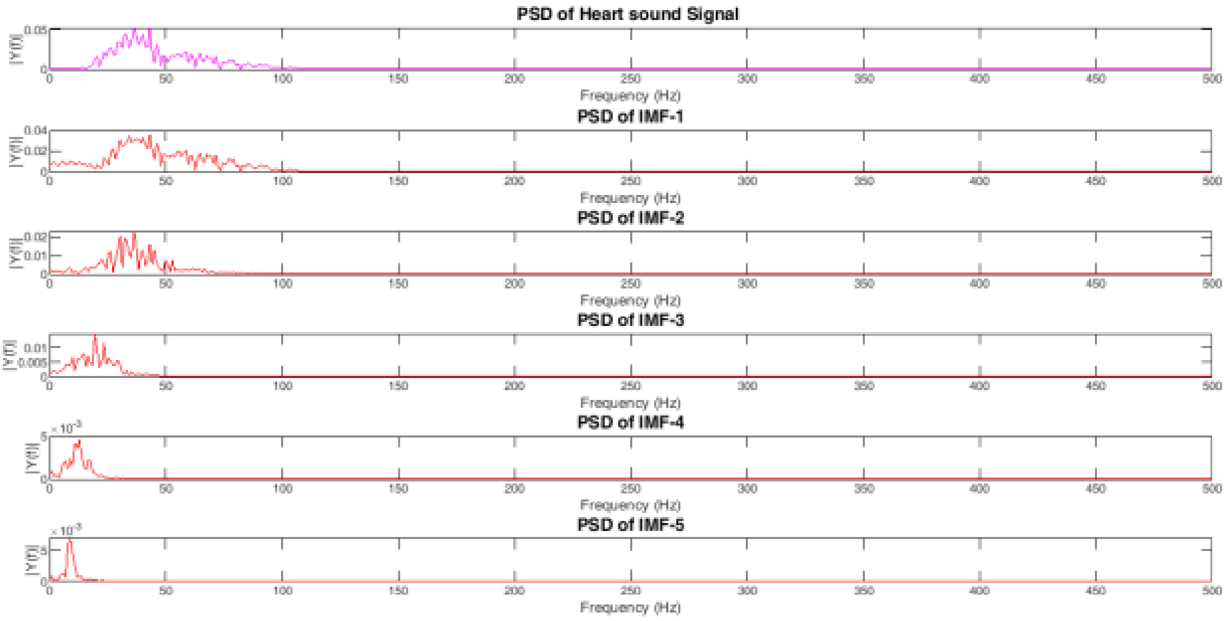

Figure 6. The frequency spectrum of heart sound signal and that of IMF-1, IMF-2, IMF-3, IMF-4 and IMF-5

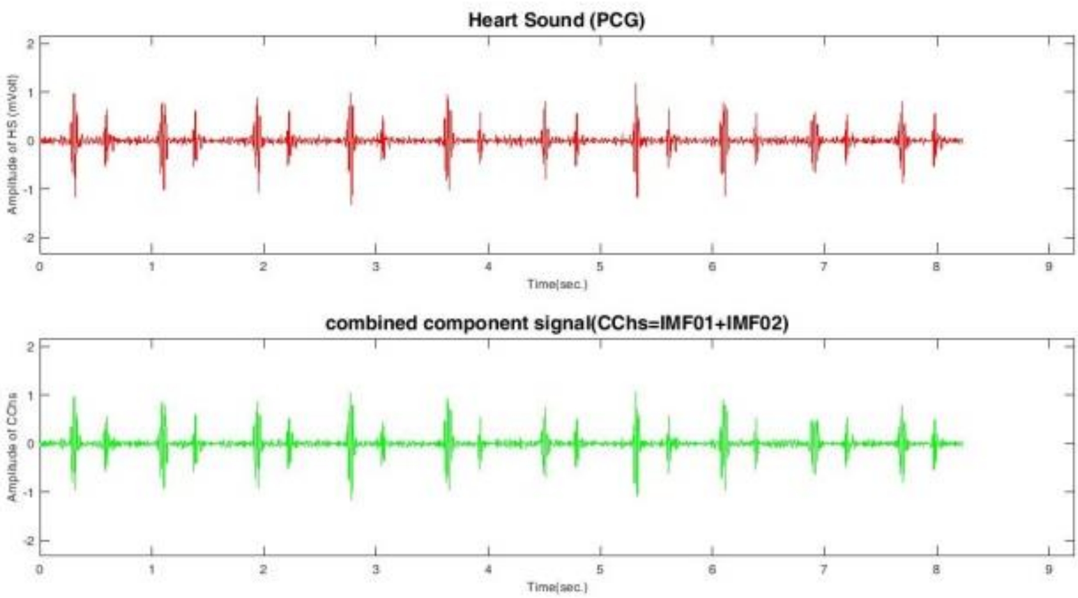

Figure 7. The PCG signal (in the upper image) and its regenerated combined component signal (CC_{hs}) in the lower-one

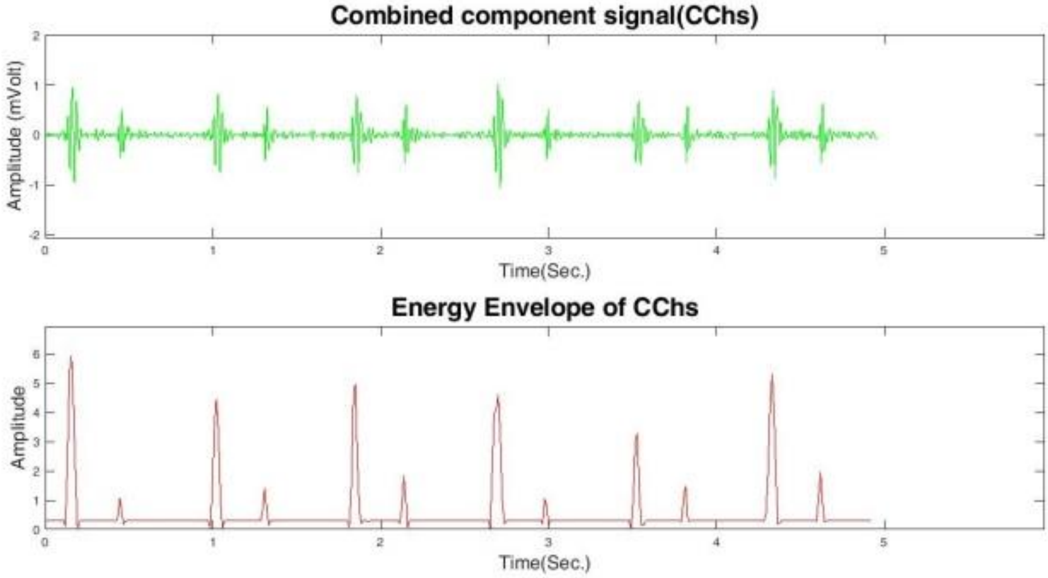

Figure 8. The combined component signal (CC_{hs}) in upper-image and its Energy envelope in the lower-image

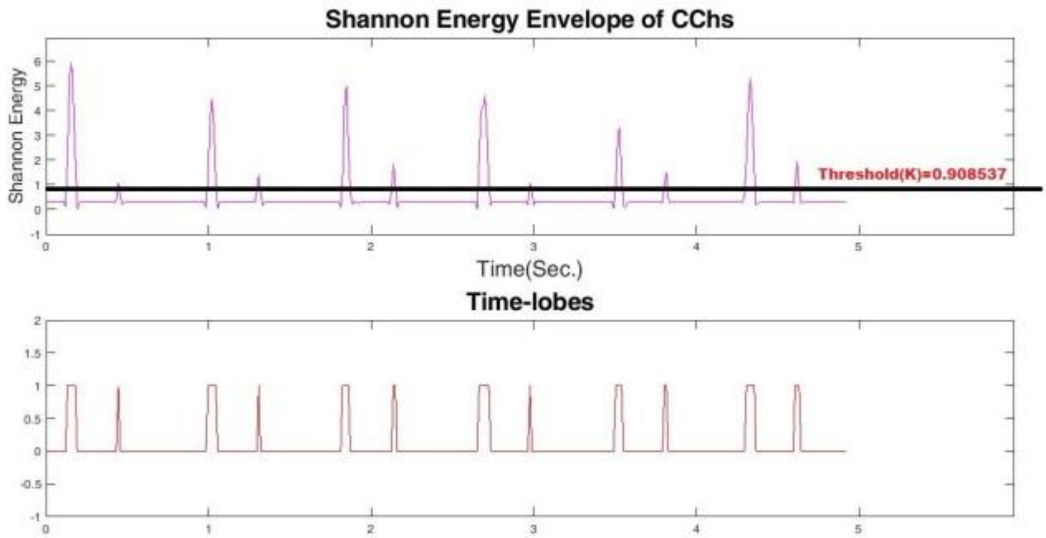

Figure 9. Thresholding of the energy envelope (in the upper-image) and the time-lobes formation after cropping by a threshold value (in the lower image)

3.1.4 Adaptive-thresholding of the energy envelope

By implementation of the MSEE method on combined component signal (CChs); the energy envelope was framed. As per Figure 8; in each cardiac cycle, two smoother peaks were observed which are representing the approximate location for identification of S_1 and S_2. Now, for creating the "time-lobes" at these locations; adaptive thresholding was used. These time-lobes could be the time-segments where the possibility of the presence of S_1 and S_2 would be highest.

By implementing the adaptive-thresholding method; a unique threshold "K" was computed for every inserted energy envelope signal. The computation of the threshold point "K" was based on cubic-spline and mean computation of energy envelope signal [3, 8]. For a particular signal, the computed threshold value (K) and the time-lobe formed are shown in Figure 9.

3.1.5 Correction of time-lobe-peaks

Sometimes, a highly noisy signal could give out false peaks of time-lobes. These false peaks of time-lobes are called here as unwanted peaks. These unwanted peaks are supposed to be false-time-lobes. Because, in a single heart-cycle; there could be appearance of two time-lobes only, using the proposed method of analysis. And, these two time-lobes would be representing the expected time-positions of first heart sound (S_1) and second heart sound (S_2) which would be detected in the further steps of the analysis. If more than two time-lobes get appeared in a single heart-cycle; then that extra time-lobe would be supposed as "unwanted peak". Because, it is well known that only two major hearts sound i.e., S_1 and S_2 occurs in a single heart-cycle and those two time-lobes would be concerned to them. In the Figure 10; there are four heart-cycles for the taken heart sound signal. Then, there is possibility of maximum 8 time-lobes. If any 9^{th} time-lobe appears, then that would be supposed as an unwanted peak. Therefore, for removal of the unwanted peaks i.e., false time-lobe-peaks; a peak correction algorithm was incorporated which was based on a modified median filtering concept [19, 20]. It improved the performance of the process to a greater extent, as shown in Figure 10.

Here, the ECG and PCG signals were simultaneously acquired from the same subjects and for the same period. So, both the signals were correlated with the same cardiac-activity-variation and had co-existence, too. In the analysis part; initially, the R-peaks of the ECG signal were detected and computed (as shown in Figure 11).

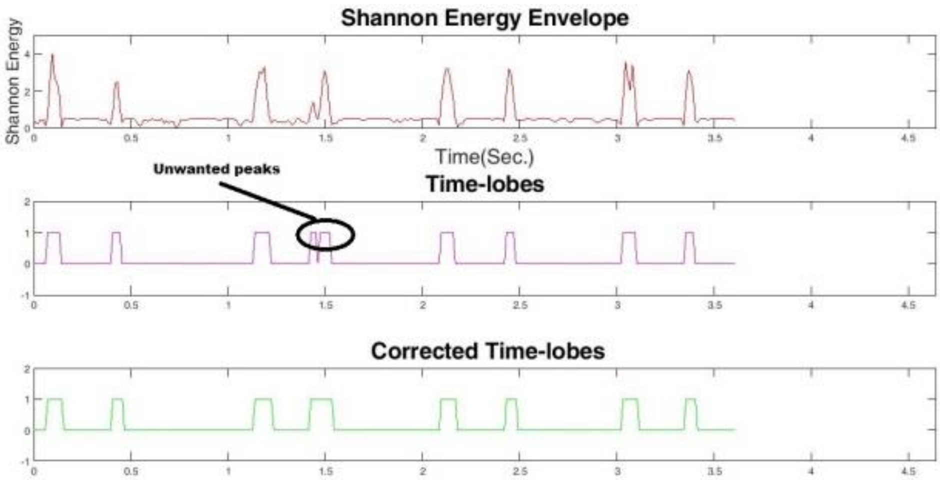

Figure 10. Time-lobe-peak correction: the energy envelope obtained from a very noisy PCG signal (in the upper image), Indicating the unwanted time-lobe-peak (in the middle image) and the corrected time-lobe-peak (in the lower image)

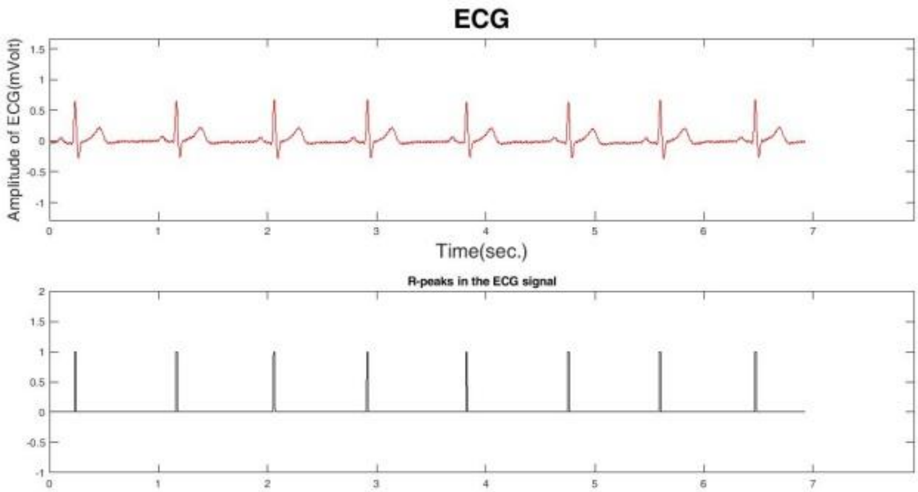

Figure 11. The original ECG signal (in the upper image) and its R-peaks (in the lower image)

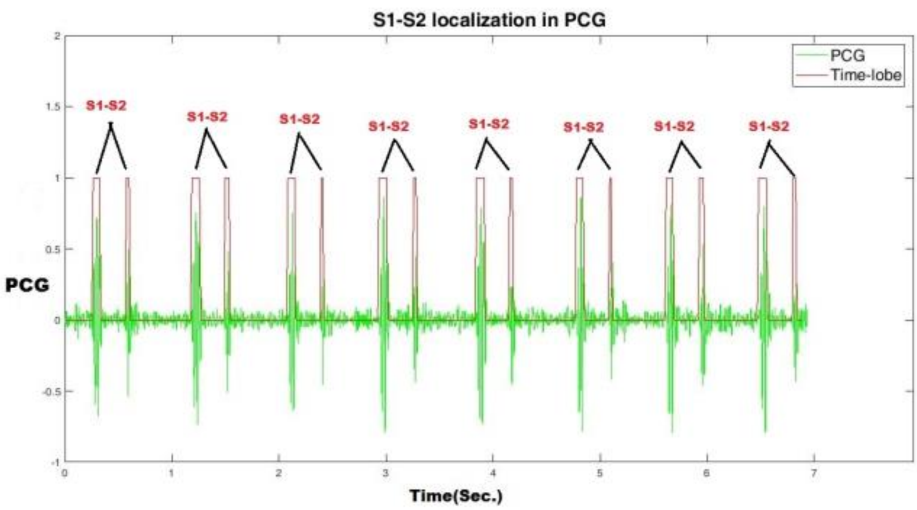

Figure 12. Localization S_1-S_2 in the PCG i.e., the time-lobes super-imposed on the positions of S_1-S_2

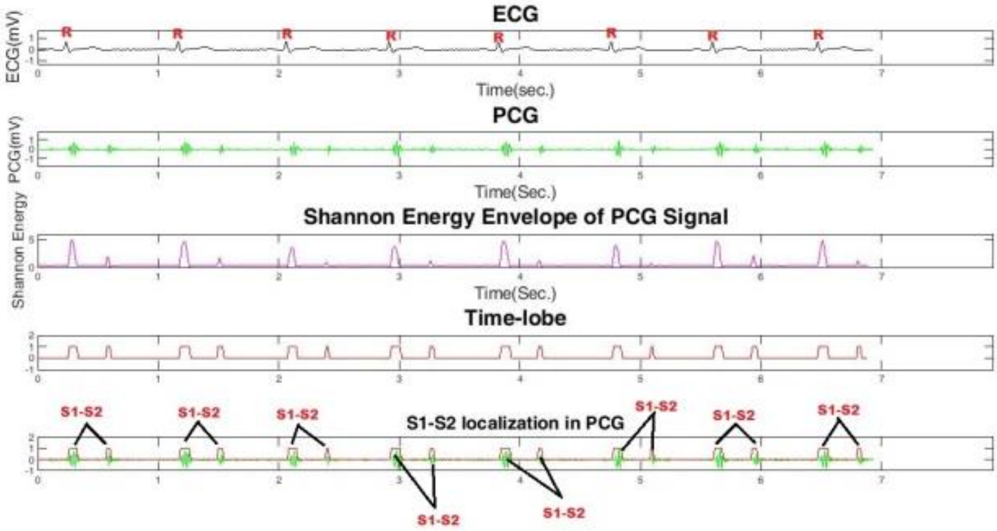

Figure 13. S_1-S_2 localization process from top to bottom: ECG with R-points (in the first image), the PCG signal (in the second image), the Shannon-energy-envelops of the PCG signal (in the third image), the time-lobes (in the fourth image), and the localization of S_1-S_2 (in the fifth image)

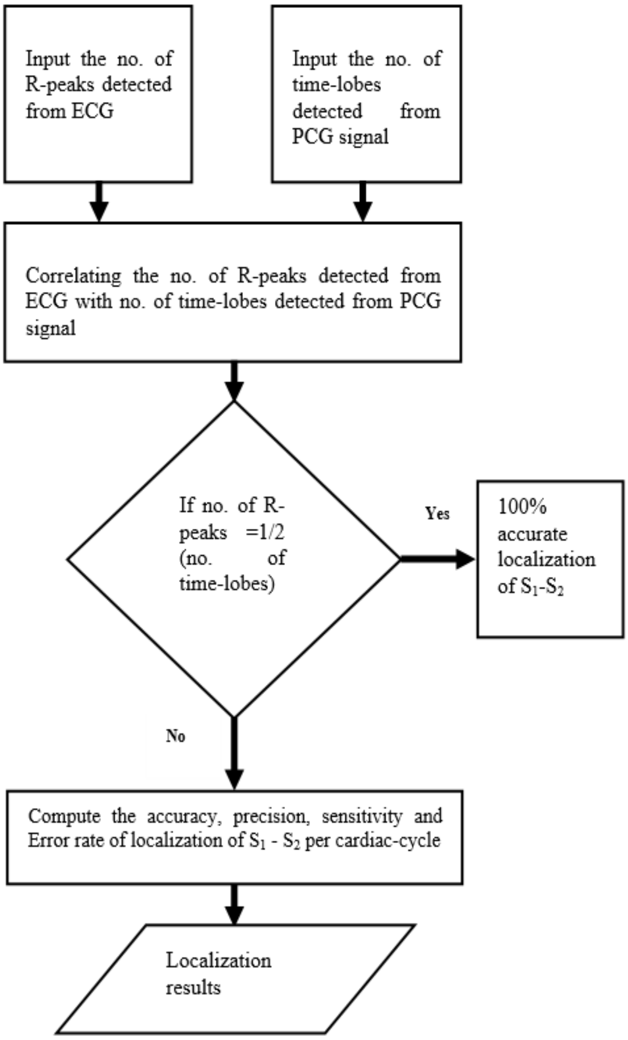

Figure 14. Decision algorithm for localization of S_1 - S_2

Then, time-lobe-peaks from combined component signal (CChs) were detected and counted using MATLAB programs. In the final stage, the computed R-peak-positions of ECG signal were made correlated with the detected quantity of time-lobe-peaks from the CChs as per the decision algorithm shown in the Figure 14. The Figure 12 is depicting the localization result of S_1-S_2 and the Figure 13 is elaborating the whole localization process in sequential manner.

Table 1. Statistics result representing accuracy of localization using the proposed method

Auscultation areas	No. of samples taken	Total no. of cardiac cycles taken	No. of cycles Successfully detected the S_1- S_2	Percentage (%) of accurate localization of S_1-S_2
Aortic(A)	10	41	24	58.54 %
Pulmonic(P)	10	51	46	90.20 %
Mitral(M)	10	51	36	70.59 %
Tricuspid(T)	10	52	36	57.69 %

Table 2. Performance evaluation of the proposed algorithm based on confusion matrix

Auscultation areas	Aortic	Pulmonic	Tricuspid	Mitral
No. of Cardiac cycles taken	41	51	51	52
TP	24	46	36	36
FP	8	05	4	10
FN	9	00	11	12
Accuracy	58.54	90.20	70.59	57.69
Precision	80.00	90.20	90.00	75.00
Sensitivity	72.72	100	76.59	71.42
Error Rate	41.46	9.8	29.41	42.31

Table 3. Assessment of the proposed algorithm with three other pre-existing methods for the PCG signal acquired from pulmonic position. Here, the proposed algorithm was compared on the basis of various parameters

	The proposed algorithm	Algorithm based on 3rd order Shannon energy [8]	Method based on heart sound envelogram [3]	Method based on Empirical mode decomposition [5]
Total heart-cycles	51	51	51	51
TP	46	43	38	35
FP	05	06	09	11
FN	00	02	04	05
Accuracy	90.20	84.31	74.51	68.62
Precision	90.20	87.75	80.85	76.08
Sensitivity	100	95.55	90.47	87.50
Error Rate	9.8	15.68	25.49	31.37

The proposed method had given a greater accuracy of localization and detection of major heart sounds, S_1 and S_2. The analysis results have been summarized in Table 1.

The summarized result of Table 1 depicts that a total of 40 samples of heart sound (PCG) consisting of total of 195 cardiac cycles were taken for the analysis. For the proposed method, it was observed that if the Pulmonic location opted for the recording of the Phonocardiogram; the accuracy of the method was found 90.20%. On the other hand, if the PCG was acquired from the remaining three auscultation areas (i.e., Tricuspid, Aortic, and Mitral), a lower success rate of detection was observed. Therefore, the Pulmonic (P) was found the best suitable position for the acquisition of heart sound signals for the analysis of S_1 and S_2.

Further, accuracy, sensitivity, precision, and Error rate metrics were used and a confusion matrix was created for the performance evaluation of the proposed algorithm. The obtained results are summarized in the Table 2, as follows [10, 21-23]:

TP = Number of cardiac cycles had 2 time-lobes, actually. And 2 time-lobes detected (concerned to S_1 and S_2), practically.

FP = Number of cardiac cycles had 2 time-lobes, actually. And more than 2 time-lobes detected, practically.

FN = Number of cardiac cycles had 2 time-lobes, actually. And less than 2 time-lobes or Zero time-lobe detected practically.

TN = Number of cardiac cycles had 2 time-lobes, actually. And zero time-lobe detected, practically. For this case, no any True Negative (TN) value was considered.

$$\text{Accuracy} = \frac{\text{TP} + \text{TN}}{\text{TP} + \text{TN} + \text{FP} + \text{FN}} \tag{4}$$

$$\text{Precision} = \frac{\text{TP}}{\text{TP} + \text{FP}} \tag{5}$$

$$\text{Sensitivity} = \frac{\text{TP}}{\text{TP} + \text{FN}} \tag{6}$$

$$\text{Error Rate} = \frac{\text{FP} + \text{FN}}{\text{TP} + \text{TN} + \text{FP} + \text{FN}} \tag{7}$$

The proposed method was compared with three other pre-existing methods. For the same self-acquired data set; the analysis approaches incorporated by Liang et al. [3], Nath et al. [8], and Bajelani et al. [5] were implemented and further depicted in Table 3.

The Table 3 depicts that the proposed approach had higher accuracy, precision, sensitivity and lower error rate for detection and localization of S_1 and S_2 as compared to pre-existing methods for the given self-acquired signal. The main advantages of the proposed method over the pre-existing methods are as following:

(a) The proposed method was analyzed and evaluated on the basis of vast number of parameters like True positive rate (TP), false positive rate (FP), false negative rate (FN), accuracy, precision, sensitivity and error rate.

(b) The database used in the proposed method of analysis was acquired or recorded by the authors by its own in a laboratory in the actual scenario. That is why it approaches to predict the much better result of analysis of real scenario.

(c) Time-lobe-correction algorithm used in the proposed method of analysis enhances the accuracy and efficiency of the proposed method.

(d) Use of the Empirical mode decomposition followed by selection of the IMFs for the reconstruction of the signal better assists in reduction of noise for the proposed method.

Moreover, it cannot be denied that the rate of success of a method not only depends upon the algorithm adopted but it also relies upon the quality of acquired data, skills of the person performing the signal acquisition, and the quality of the instruments/machines used in the acquisition process [24-29]. Hence, if more standard databases would be used for the proposed method, the accuracy would be higher.

4. CONCLUSIONS

For the human body, regular monitoring of cardiac health could reduce the possibility of an attack of a fatal disease. The monitoring of the health of the heart is mainly accomplished by the monitoring of the ECG. But there could be a few symptoms of heart disease like heart-valve-dysfunction that could not be reflected exactly in the ECG signal. Therefore, in the diagnosis of cardio-health, specifically concerned with heart-valve-dysfunction; the monitoring of the PCG signal plays a vital role. Generally, there could be two prime sounds that come out in a single cycle of the PCG signal which could be identified as S_1 and S_2. These two heart sounds consist of a large extent of information because of their higher amplitude. The remaining two heart sounds i.e., S_3 and S_4 consist of lower amplitude and gets merged with the heart murmurs and the other noises. Therefore, analysis of S_1 and S_2 was focused, here.

By placing an electronic stethoscope on the four different specific points of the human chest, the PCG signal was recorded. The ECG signal was also acquired, simultaneously, to be used as a reference of the cardiac cycle. After the sample preparation and denoising of the signal, the PCG signal was decomposed into its frequency components using Empirical Mode Decomposition (EMD). Further, two frequency components (IMF-1 and IMF-2) were chosen and recombined to reconstruct the signal for the upcoming steps of the analysis. Choosing the first two IMFs intensified the frequency components concerned to S_1 and S_2 in the signal and reduced the computation cost, too. It also helped to discard the low-frequency noises and high-frequency artifacts from the signal. Finally, the Modified Shannon Energy Envelope algorithm (MSEE) i.e., 4th order Shannon Energy Envelope approach was implemented followed by adaptive thresholding and time-lobe correction algorithm for the localization and detection of S_1 and S_2.

The final analysis result depicted that for the self-acquired PCG signal from the Pulmonic position; the proposed method revealed the accuracy and the precision 90.20%, the sensitivity 100%, and the error rate 9.8%. Thereafter, the proposed approach was compared with three other pre-existing approaches for the same self-acquired signals and it was found that the proposed approach had greater accuracy of localization of S_1 and S_2.

REFERENCES

[1] Cardiovascular Disease: Key facts, https://www.who.int/news-room/factsheets/detail/cardiovascular-diseases-cvds, accessed on 11 Jan 2022.

[2] Cardiovasculardiseasesdiseases. (2021). https://www.who.int/india/health-topics/cardiovascular-diseases, accessed on 11 Jan 2022.

[3] Liang, H., Lukkarinen, S., Hartimo, I. (1997). Heart sound segmentation algorithm based on heart sound envelogram. In Computers in Cardiology 1997, IEEE, pp. 105-108. https://doi.org/10.1109/CIC.1997.647841

[4] Belmecheri, M.Z., Ahfir, M., Kale, I. (2018). Automatic heart sounds segmentation based on the correlation coefficients matrix for similar cardiac cycles identification. Biomedical Signal Processing and Control, 43: 300-310. https://doi.org/10.1016/j.bspc.2018.03.009

[5] Bajelani, K., Navidbakhsh, M., Behnam, H., Doyle, J.D., Hassani, K. (2013). Detection and identification of first and second heart sounds using empirical mode decomposition. Proceedings of the Institution of Mechanical Engineers, Part H: Journal of Engineering in Medicine, 227(9): 976-987. https://doi.org/10.1177/0954411913493734

[6] Nath M. Heart sound delineation and time-frequency analysis. M Tech Thesis, National Institute of Technology, Jalandhar, India, 2010.

[7] Narváez, P., Gutierrez, S., Percybrooks, W.S. (2020). Automatic segmentation and classification of heart sounds using modified empirical wavelet transform and power features. Applied Sciences, 10(14): 4791. https://doi.org/10.3390/app10144791

[8] Nath, M., Srivastava, S., Kulshrestha, N., Singh, D. (2021). Detection and localization of S_1 and S_2 heart sounds by 3rd order normalized average Shannon energy envelope algorithm. Proceedings of the Institution of Mechanical Engineers, Part H: Journal of Engineering in Medicine, 235(6): 615-624. https://doi.org/10.1177/0954411921998108

[9] Liu, Q., Wu, X., Ma, X. (2018). An automatic segmentation method for heart sounds. Biomedical Engineering Online, 17: 1-22. https://doi.org/10.1186/s12938-018-0538-9

[10] Akram, M.U., Shaukat, A., Hussain, F., Khawaja, S.G., Butt, W.H. (2018). Analysis of PCG signals using quality assessment and homomorphic filters for localization and classification of heart sounds. Computer Methods and Programs in Biomedicine, 164: 143-157. https://doi.org/10.1016/j.cmpb.2018.07.006

[11] Giordano, N., Knaflitz, M. (2019). A novel method for measuring the timing of heart sound components through digital phonocardiography. Sensors, 19(8): 1868. https://doi.org/10.3390/s19081868

[12] Abbas, A.K., Bassam, R. (2009). Phonocardiography signal processing. Synthesis Lectures on Biomedical Engineering, 4(1): 1-194.

[13] Delgado-Trejos, E., Quiceno-Manrique, A.F., Godino-Llorente, J.I., Blanco-Velasco, M., Castellanos-Dominguez, G. (2009). Digital auscultation analysis for heart murmur detection. Annals of Biomedical Engineering, 37: 337-353. https://doi.org/10.1007/s10439-008-9611-z

[14] Hanna, I.R., Silverman, M.E. (2002). A history of cardiac auscultation and some of its contributors. The American Journal of Cardiology, 90(3): 259-267. https://doi.org/10.1016/S0002-9149(02)02465-7

[15] Ismail, S., Siddiqi, I., Akram, U. (2018). Localization and classification of heart beats in phonocardiography signals-a comprehensive review. EURASIP Journal on Advances in Signal Processing, 2018(1): 1-27. https://doi.org/10.1186/s13634-018-0545-9

[16] Life science signals & physiological measurements (2020) Biopac. https://www.biopac.com/physiological-signals-biopac.

[17] Boutana, D., Barkat, B., Benidir, M. (2013). Segmentation of pathological heart sound signal using empirical mode de composition. International Journal of Computer and Electrical Engineering, 5(1): 26. https://doi.org/10.7763/IJCEE.2013.V5.655

[18] Debbal, S.M., Bereksi-Reguig, F. (2008). Computerized heart sounds analysis. Computers in Biology and Medicine, 38(2): 263-280. https://doi.org/10.1016/j.compbiomed.2007.09.006.

[19] Kalaimani, G., Manojkumar, K., Kumar, S.S. (2019). Median filtering for removal of maximum impulse noise from images with a decision based model. Journal of Computational and Theoretical Nanoscience, 16(2): 562-567. https://doi.org/10.1166/jctn.2019.7769

[20] Stone, D.C. (1995). Application of median filtering to noisy data. Canadian Journal of Chemistry, 73(10): 1573-1581. https://doi.org/10.1139/v95-195

[21] Kumar, A., Srivastava, S. (2022). Restoration and enhancement of breast ultrasound images using extended complex diffusion based unsharp masking. Proceedings of the Institution of Mechanical Engineers, Part H: Journal of Engineering in Medicine, 236(1): 12-29. https://doi.org/10.1177/09544119211039317

[22] Kumar, V., Srivastava, S. (2022). Performance analysis of reshaped Gabor filter for removing the Rician distributed noise in brain MR images. Proceedings of the Institution of Mechanical Engineers, Part H: Journal of Engineering in Medicine, 236(8): 1216-1231. https://doi.org/10.1177/09544119221105690

[23] Kumar, P., Kumar, A., Srivastava, S., Padma Sai, Y. (2022). A novel bi-modal extended Huber loss function based refined mask RCNN approach for automatic multi instance detection and localization of breast cancer. Proceedings of the Institution of Mechanical Engineers, Part H: Journal of Engineering in Medicine, 236(7): 1036-1053. https://doi.org/10.1177/09544119221095416

[24] Marcus, G., Vessey, J., Jordan, M.V., Huddleston, M., Keown, B., Gerber, I. L., Foster, E., Chatterjee, K., McCulloch, C.E., Michaels, A.D. (2006). Relationship between accurate auscultation of a clinically useful third heart sound and level of experience. Archives of Internal Medicine, 166(6): 617-622. https://doi.org/10.1001/archinte.166.6.617

[25] Huiying, L., Sakari, L., Iiro, H. (1997). A heart sound segmentation algorithm using wavelet decomposition and reconstruction. In Proceedings of the 19th Annual International Conference of the IEEE Engineering in Medicine and Biology Society. 'Magnificent Milestones and Emerging Opportunities in Medical Engineering'(Cat. No. 97CH36136), 4: 1630-1633. https://doi.org/10.1109/IEMBS.1997.757028

[26] Barma, S., Chen, B.W., Ji, W., Rho, S., Chou, C.H., Wang, J.F. (2015). Detection of the third heart sound based on nonlinear signal decomposition and time-frequency localization. IEEE Transactions on Biomedical Engineering, 63(8): 1718-1727. https://doi.org/10.1109/TBME.2015.2500276

[27] Moukadem, A., Dieterlen, A., Hueber, N., Brandt, C. (2013). A robust heart sounds segmentation module based on S-transform. Biomedical Signal Processing and Control, 8(3): 273-281. https://doi.org/10.1016/j.bspc.2012.11.008

[28] Alexander, B., Nallathambi, G., Selvaraj, N. (2018). Screening of heart sounds using hidden Markov and Gammatone filterbank models. In 2018 17th IEEE International Conference on Machine Learning and Applications (ICMLA), pp. 1460-1465. https://doi.org/10.1109/ICMLA.2018.00237

[29] Abdollahpur, M., Ghaffari, A., Ghiasi, S., Mollakazemi, M.J. (2017). Detection of pathological heart sounds. Physiological Measurement, 38(8): 1616. https://doi.org/10.1088/1361-6579/aa7840